

## Self-Assembly of Particles for Densest Packing by Mechanical Vibration

A. B. Yu,<sup>\*</sup> X. Z. An, R. P. Zou, R. Y. Yang, and K. Kendall<sup>†</sup>

Center for Simulation and Modeling of Particulate Systems, School of Materials Science and Engineering,  
The University of New South Wales, Sydney, New South Wales 2052, Australia

(Received 9 August 2006; published 26 December 2006)

It is shown that by properly controlling vibrational and charging conditions, the transition from disordered to ordered, densest packing of particles can be obtained consistently. The method applies to both spherical and nonspherical particles. For spheres, face centered cubic packing with different orientations can be achieved by monitoring the vibration amplitude and frequency, and the structure of the bottom layer, in particular. The resultant force structures are ordered but do not necessarily correspond to the packing structures fully. The implications of the findings are also discussed.

DOI: 10.1103/PhysRevLett.97.265501

PACS numbers: 61.43.Gt, 61.43.Bn, 81.05.Rm

One of the most fundamental questions in self-assembly of particles is how to achieve the densest possible geometrical ordering [1–3]. Theoretically, face centered cubic (fcc) or hexagonal close packing (hcp) with packing density  $\rho = \pi/3\sqrt{2} \approx 0.74$  gives the densest structure, and this hypothesis, known as the Kepler conjecture, has been recently justified [4,5]. For atoms, this structure can be observed for various materials, formed naturally as a result of the interaction of different atomic forces. However, for mesoparticles, it is not clear how to obtain this packing state consistently. When poured in a container to form a packing under gravity, spheres give  $\rho \approx 0.60$  [6]. This value varies slightly depending on material properties and other dynamic variables [2,7]. Any further increase in  $\rho$  requires external energy to overcome the interparticle locking or jamming. Vibration is a method to do so. One-dimensional (1D) vibration in the vertical direction can lead to some particle rearrangements, increasing  $\rho$  to 0.64 [8–10]. Any further increase is difficult to achieve. This is also the case when compaction applies [11]. However, it is recently found that two- (2D) or three-dimensional (3D) vibration, or other packing methods such as shearing can increase  $\rho$  to about 0.68 [12–14]. Local crystallization, which may be related to fcc or hcp, has also been observed [14,15]. However, the overall  $\rho$  obtained is still much lower than 0.74 except for the work of Blair *et al.* [16] and Nahmad-Molinari and Ruiz-Suarez [17] who produced hcp with some manual arrangement of spheres. The difficulty to generate reproducible results without human intervention suggests that factors controlling the formation of the densest packing are not properly understood.

In this work, we have studied the packing of particles with the following two methods: (I) Packing followed by vibration: By this method, spheres are first poured into a container to form a packing. Then, vibration is applied, which can be 1D (vertical), 2D (horizontal), or 3D (vertical and horizontal). (II) Simultaneous packing and vibration: This method differs from the above by adding spheres into a container batch by batch. Packing and vibration effect

simultaneously. One more variable introduced is the weight of each batch.

Glass beads of diameter  $d = 3$  mm were used in our experiments which involved gentle vibration and the so-called double extrapolation method to avoid the wall effect [6,18]. Thus, cylindrical containers of different diameter  $D$  were used and for each experiment,  $\rho$  was determined from the bead height in a container (measurement error is within 0.5 mm). For brevity, we here only give the results showing the relationship between  $\rho$  and  $d/D$  ratio. Figure 1 indicates that the improvement in the degree of freedom, here achieved by increasing the dimension in vibration, can increase  $\rho$ . When method I is used, 1D vibration can only increase  $\rho$  to  $\rho_{\max} = 0.64$ , corresponding to the well known random close packing (rcp) [6,10,19]. 2D or 3D vibration can increase  $\rho$  to 0.655 or 0.661, respectively, consistent with the recent finding that  $\rho > 0.64$  is possible

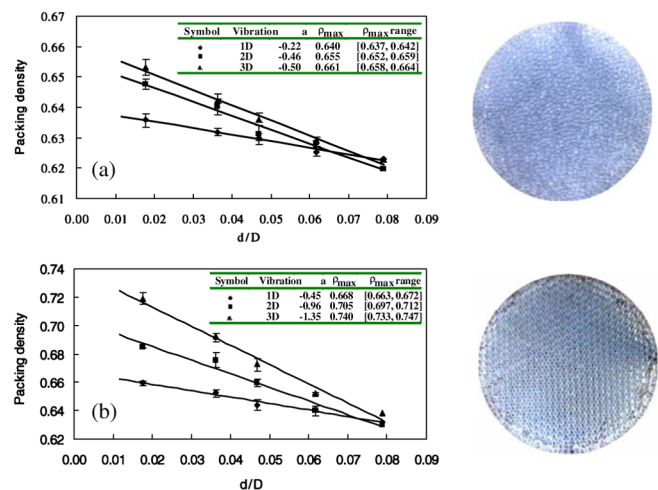


FIG. 1 (color online).  $\rho$  as a function of  $d/D$  ratio under different conditions: (a), method I; and (b), method II. The results are fitted by a linear equation  $\rho = a \times (d/D) + \rho_{\max}$ , and parameters  $a$  and  $\rho_{\max}$ , together with the varying range of  $\rho_{\max}$  when the level of confidence is 95%, are listed. The right photos (top view) were taken when  $d/D = 0.036$ .

if conditions are right [12–14]. We believe that the so-called rcp is a packing limit when the motion of particles is highly 1D. If spheres are allowed to move two- or three-dimensionally, this limit can be overcome. Jamming or arching does exist among spheres restricting the rearrangement of spheres. It corresponds to the force network among spheres formed in the motion of multisphere system. An effective way to prevent jamming is to use a batchwise addition of spheres to form a packing, i.e., method II here. In this case, newly added spheres have enough time to organize themselves to form a stable dense packing. If batch weight is small enough, arching may be fully eliminated. Consequently,  $\rho$  can be increased. This is indeed the case as shown in Fig. 1(b). The fact that  $\rho > 0.64$  even for 1D vibration is because 2D or 3D motion occurs to the newly added particles under the present method II conditions. 2D/3D motion of particles may also be induced in the work of Nowak *et al.* [13]. Most importantly, we found that the extrapolated  $\rho_{\max}$  as high as 0.74 can be achieved when 3D vibration is used. Crystallization is obvious, although it is disturbed by wall [Fig. 1(b) inset]. In contrast, crystallization is not clearly observed when method I is used [Fig. 1(a) inset].

This packing method can also produce densest packing for nonspherical particles. For example, for cubes, we obtained  $\rho_{\max} \approx 1$ , and interestingly 1D, 2D, and 3D vibrations produced comparable results.  $\rho = 1$  is actually the theoretical limit for particle packing. It can be obtained only for cubelike particles which can fully eliminate the voids among particles when packed in an ordered manner. Disordered packing formed by cubes under the conventional loose and dense packing conditions produces a much lower packing density [1,18].

To produce results for better understanding, we then conducted numerical simulations by means of the dynamic simulation technique. The technique has been extensively used in our previous study of particle packing and flow [20]. The simulation conditions for this work are similar to the experiments. However, to eliminate the (side) wall effect, periodic boundary conditions were used in both horizontal directions (the container is rectangular, typically with a width of  $12d$ ). So vibration was realized by monitoring the motion of the bottom wall supporting the spheres (we assumed that the container has the same physical properties as spheres). The parameters used for spheres were the same as those used in our work for glass beads [10,21,22]. As a dynamic process, many variables including the deposition condition (e.g., deposition position) and material properties [7] may affect the packing behavior. In the present work, we added particles randomly in position at a height of  $30d$  above the container bottom and only considered three variables, i.e., vibration amplitude  $A$  and frequency  $\omega$ , and if applicable, batch weight (expressed as the number of spheres per batch  $N_p$ ). In a case involving 2D or 3D vibration,  $A$  and  $\omega$  were assumed to be the same in all directions. We calculated  $\rho$  and analyzed the structure for a central section of bed to eliminate the wall effect,

as done elsewhere [10]. The number of spheres varies from 2500 to 10 000. The low value was used in most of the simulations.

Figure 2 shows an example involving all operations. It demonstrates the evolution of  $\rho$  during a 3D vibration when method II was used and vibration stopped after every 1 s to add spheres onto the packing formed and produce a stable packing. Two regions can be identified from Fig. 2. The first region is until about 28 s, where  $\rho$  increases with time. The fluctuation observed corresponds to the vibration which compresses and relaxes the packing periodically. In the second region, vibration loosens packing but  $\rho$  simply fluctuates in the same pattern. Because of the elimination of the side wall effect, except for the top few layers of particles, convective flow with relative motion between particles is not observed. When vibration stops, spheres gradually settle down to form a stable packing. Such curves were observed for all the simulations conducted, although  $\rho$  varies with operational conditions. For this particular case,  $\rho = 0.739$  for the final packing, very close to fcc or hcp. Another way to form a packing is adding spheres at a preset rate while vibrating the bed.  $\rho$  obtained by this method is usually lower if the other conditions are the same. For example, when the packing conditions were the same as those for Fig. 2 (the adding rate is 98 particles/second to correspond to  $N_p = 98$  particles/batch),  $\rho = 0.728$  was obtained.

Many simulations have been done but here we are only focused on the most important findings related to the experiments. Figure 3 shows the results obtained under different vibrational conditions. It indicates that  $\rho$  increases to a maximum and then decreases with  $A$  for a constant  $\omega$ . The maximum packing density  $\rho_{\max}$  should be obtained by properly controlling  $A$  and  $\omega$ . It is 0.64 or 0.651 under 1D or 3D vibration for method I, and 0.658 or 0.739 under 1D or 3D vibration for method II. They are consistent with the experimental results. However, 2D vibration does not result in any significant change in  $\rho$ .

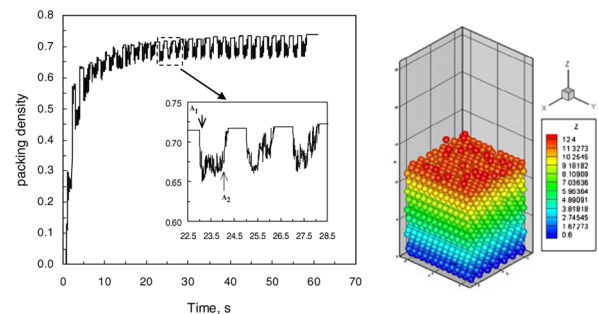


FIG. 2 (color online). Evolution of  $\rho$  when  $A = 0.1d$ ,  $\omega = 200$  rad/s, and  $N_p = 98$  particles/batch (method II). For each operational cycle,  $A_1$  represents the addition of spheres and start of vibration, and  $A_2$  the end of vibration. Note that the addition of spheres stops at 25 s, although the whole packing process ends at  $t = 59$  s to produce the final stable packing. The right figure is a snapshot showing the formation of the packing.

This is because in the simulation, the side wall and its promoted particle rearrangement were eliminated. The horizontal motion of the bottom wall could not excite the particles in a packing except for a few layers at the bottom. Figure 3(b) also indicates that over a relatively large range of  $A$ ,  $\rho$  does not change much under 1D vibration when method II is used. This phenomenon is not always so; the change of vibration conditions and batch weight may result in different behavior.

In fact, batch weight  $N_p$  plays a critical role in achieving the densest packing. This is clearly shown in Fig. 4(a), where three regions can be identified. In region III ( $N_p > 350$  particles/batch), a packing forms similarly to that when method I is used, and vibration does not result in any significant change in  $\rho$ . In region II ( $200 < N_p \leq 350$  particles/batch),  $\rho$  increases with the decrease of  $N_p$ , as a result of the decreased probability of forming arches among particles. In region I ( $N_p \leq 200$  particles/batch, which is around the number of spheres required to produce one layer of particles in a packing), the densest packing can be consistently obtained.

Our results clearly show that  $\rho = 0.74$  is achievable. What is the corresponding packing structure, fcc or hcp? To clarify this matter, we analyzed samples from the inner packing and found they are fcc. This agrees with the theoretical consideration that fcc is more stable than hcp for naturally formed packings [23], although stable hcp may be produced under special conditions [16,17]. Moreover, as shown in Fig. 4(a) (insets), two different orientations of fcc are possible:  $\{100\}$  and  $\{111\}$ . Such structures, particularly the  $\{100\}$  oriented fcc, can also be produced by slow sedimentation of colloidal particles in the so-called colloidal epitaxy process [24]. They are here obtained under different vibrational conditions. The  $\{100\}$  oriented fcc is obtained when  $A = 0.2d$ ,  $\omega = 200$  rad/s and  $N_p = 101$  particles/batch, and the  $\{111\}$  oriented fcc is obtained when  $A = 0.1d$ ,  $\omega = 200$  rad/s and  $N_p = 98$  particles/batch. For each sphere in the  $\{100\}$  oriented fcc, it is in contact with 12 spheres, with 4 at underneath, horizontal, and above levels, respectively. Vertically, it gives an ABAB... pattern; note that this pattern does not

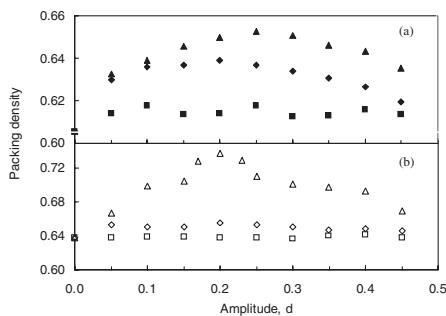


FIG. 3. Particle density as a function of vibration amplitude under 1D ( $\blacklozenge$ ,  $\diamond$ ), 2D ( $\blacksquare$ ,  $\square$ ), and 3D ( $\blacktriangle$ ,  $\triangle$ ) conditions: (a), method I when  $\omega = 100$  rad/s; (b), method II when  $\omega = 200$  rad/s,  $N_p = 101$  particles/batch.

mean the structure is hcp because one of the two alternative layers is not hexagonal in structure. The  $\{111\}$  oriented fcc gives quite different contacts: 6 at horizontal level, and 3 at underneath and above levels, respectively. Vertically, it has an ABCABC... pattern.

The formation of the first bottom layer appears to be most critical to the final structure. To test this idea, we fixed this layer using hexagonal or cubic arrangement and then change the vibration conditions. The results suggest that the hexagonal arrangement can lead to  $\{111\}$  oriented fcc even when  $A = 0.2d$ ,  $\omega = 200$  rad/s and  $N_p = 101$  particles/batch, the conditions leading to the  $\{100\}$  oriented fcc as mentioned above. On the other hand, the cubic arrangement at the bottom layer leads to  $\{100\}$  oriented fcc. In theory, hexagonal arrangement is more stable than cubic for each layer. Consequently,  $\{111\}$  oriented fcc should be more stable than  $\{100\}$  oriented fcc. This fcc orientation is also favored in the experiments [Fig. 1(b) inset, and also from our dissection examination of the packing structure layer by layer]. The analysis of the simulated structures indicates that both fcc and hcp can form locally once  $\rho$  is greater than about 0.6, but the hcp proportion reaches its maximum at  $\rho = 0.70$  and vanishes at  $\rho = 0.74$ .

One advantage of the present simulation technique is that not only the structure but also the forces acting on particles can be obtained [10,21,22]. We have analyzed the forces with special reference to the normal forces between particles as done elsewhere [10,21]. As shown in Figs. 4(b) and 4(c), different orientations give different force structures. For the  $\{100\}$  oriented fcc, force chains develop vertically at two angles  $\pi/4$  and  $3\pi/4$  (front view) to counteract gravity. A sphere is supported by 4 underneath spheres and supports other 4 above, and there is no need to have horizontal forces to maintain stability. For the  $\{111\}$  oriented fcc, force chains also develop vertically, but at angles  $\pi/5$  and  $4\pi/5$ . Notably, strong horizontal forces exist. The horizontal forces provide a strong force “jamming” making the  $\{111\}$  orientated fcc mechanically more

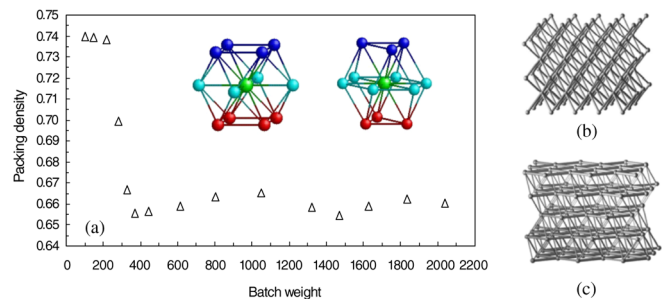


FIG. 4 (color online). (a) Influence of  $N_p$  on  $\rho$  when  $A = 0.1d$ ,  $\omega = 200$  rad/s. The insets show the representative structure for: left,  $\{100\}$ ; and right,  $\{111\}$  oriented fcc, obtained when  $N_p$  is small enough with different  $A$  and  $\omega$ . (b) and (c) show, respectively, the force structure of the  $\{100\}$  and  $\{111\}$  oriented fcc, where each line represents a normal contact force between spheres whose centers are shown by small spheres, with its thickness proportional to its magnitude.

stable. Interestingly, although there are 6 horizontal contacts, only 4 forces are required to maintain stability, with 2 forces negligible. So a sphere has 10 normal contact forces in the  $\{111\}$  orientated fcc, against 8 in the  $\{100\}$  orientated fcc.

Figures 4(b) and 4(c) also demonstrate that the force structure is ordered. The results present evidence to support the theoretical efforts often assuming ordered force patterns for ordered packing structure [25,26]. However, the force structure of a packing does not necessarily correspond on its packing structure fully. Packing and force structures both depend on many variables related to material properties and packing method, and the history of formation as well. They offer critical information to assess information propagation in granular solids [27]. At this stage of development, experimental techniques only allow the measurements of the forces at a wall or boundary of a particle assembly [28,29]. Numerical simulations can overcome this limit but need validation. Further studies are certainly necessary in this area.

The motion of particles is governed by various forces between particles in addition to gravity. It is deterministic at a particle scale. However, the final positions of particles in a system depend on the equilibrium of the forces which associates with the random motion at a larger, if not global, scale. Consequently, the whole packing structure may not be a perfect fcc. In fact, local defect was observed in this work. Because of this, our packing gives a packing density slightly lower. The difference can also be observed at a microstructural level, for example, in our analysis of the radial and angular distribution functions. How to develop a method to fully eliminate the defects is an important research area to be carried out in the future.

In summary, we showed that by properly controlling vibrational conditions, the densest packing can be obtained consistently. The method appears to apply to not only spheres but also nonspherical particles. The driving force for self-assembly is an external mechanical force, which is different from the systems studied by Whitesides and colleagues [30], and can be used more conveniently. For spheres,  $\{100\}$  and  $\{111\}$  oriented fccs can be produced by monitoring vibration amplitude and frequency, and the structure of the bottom layer, in particular. The method may open a new, dense packing system which needs extensive research in order to understand the effects of variables related to particle characteristics, material properties and packing method, and control particle packing for different practical needs. Such control is important to materials and other industries whose final particulate products are very much related to the packing structure [1]. Moreover, sphere packing has been widely used to model various important phenomena in nature, e.g., liquid structure, and phase transition in glassy and/or colloidal system [2]. However, such studies are handicapped because of the difficulty in producing packings of density significantly higher than 0.64. This difficulty can now be readily overcome with the packing method proposed.

We are grateful to the Australian Research Council for the financial support of this work.

\*Corresponding author.

Email address: a.yu@unsw.edu.au

†On sabbatical leave from Dept. of Chemical Engineering, Univ. of Birmingham, Birmingham, U.K.

- [1] R.M. German, *Particle Packing Characteristics* (Metal Powder Industries Federation, Princeton, New Jersey, 1989).
- [2] D. Bideau and A. Hansen, *Disorder and Granular Media*, edited by H.E. Stanley and E. Guyon (Elsevier Science Publishers, North-Holland, Amsterdam, 1993).
- [3] C. Zong, *Sphere Packings* (Springer, New York, 1999).
- [4] T.C. Hales, *Discrete Comput. Geom.* **17**, 1 (1997); also see <http://lanl.arxiv.org/abs/math.MG/9811071> for "An Overview of the Kepler Conjecture."
- [5] G.G. Szpiro, *Kepler's Conjecture: How Some of the Greatest Minds in History Helped Solve One of the Oldest Math Problems in the World* (Wiley, New York, 2003).
- [6] G.D. Scott, *Nature (London)* **188**, 908 (1960).
- [7] Z.P. Zhang, L.F. Liu, and A.B. Yu, *Powder Technol.* **116**, 23 (2001).
- [8] J.E. Ayer and F.E. Soppet, *J. Am. Ceram. Soc.* **48**, 180 (1965).
- [9] J.B. Knight *et al.*, *Phys. Rev. E* **51**, 3957 (1995).
- [10] X.Z. An *et al.*, *Phys. Rev. Lett.* **95**, 205502 (2005).
- [11] K. Kawakita and K.-H. Ludde, *Powder Technol.* **4**, 61 (1971).
- [12] O. Pouliquen, M. Nicolas, and P.D. Weidman, *Phys. Rev. Lett.* **79**, 3640 (1997).
- [13] E.R. Nowak *et al.*, *Phys. Rev. E* **57**, 1971 (1998).
- [14] K.E. Daniels and R.P. Behringer, *Phys. Rev. Lett.* **94**, 168001 (2005).
- [15] T.G. Oweberg, R.L. McDonald, and R.J. Trainor, *Powder Technol.* **3**, 183 (1970).
- [16] D.L. Blair *et al.*, *Phys. Rev. E* **63**, 041304 (2001).
- [17] Y. Nahmad-Molinari and J.C. Ruiz-Suarez, *Phys. Rev. Lett.* **89**, 264302 (2002).
- [18] R.P. Zou and A.B. Yu, *Powder Technol.* **88**, 71 (1996).
- [19] K. Gotoh and J.L. Finney, *Nature (London)* **252**, 202 (1974).
- [20] A.B. Yu, *Eng. Comput.* **21**, 205 (2004).
- [21] R.Y. Yang, R.P. Zou, and A.B. Yu, *Phys. Rev. E* **62**, 3900 (2000).
- [22] K.J. Dong *et al.*, *Phys. Rev. Lett.* **96**, 145505 (2006).
- [23] L.V. Woodcock, *Nature (London)* **385**, 141 (1997).
- [24] A. van Blaaderen, R. Ruel, and P. Wiltzius, *Nature (London)* **385**, 321 (1997).
- [25] S.F. Edwards and C.C. Mountfield, *Physica (Amsterdam)* **226A**, 25 (1996).
- [26] C. Goldenberg and I. Goldhirsch, *Nature (London)* **435**, 188 (2005).
- [27] S. Luding, *Nature (London)* **435**, 159 (2005).
- [28] C.H. Liu *et al.*, *Science* **269**, 513 (1995).
- [29] T.S. Majmudar and R.P. Behringer, *Nature (London)* **435**, 1079 (2005).
- [30] G.M. Whitesides and B. Grzybowski, *Science* **295**, 2418 (2002); also T.L. Breen *et al.*, *Science* **284**, 948 (1999).